

# Electric Field and Thermal Properties of Wet Cable: Using FEM

Sushman Kumar Kanikella

Dept of Electrical and Electronics Engg, NITK, Surathkal, Mangalore, Karnataka, India

E-mail: sushman254@gmail.com

## Abstract

A Single phase medium voltage power cable (XLPE) buried in soil and it can be used to investigate electric field, potential distribution and increased temperature of the cable insulation with rising load currents, are known to accelerate the formation of water and electric trees in cables which ultimately lead to cables failure. To determine the thermal and electrical behavior of a given wet cable installation. The work presented in this paper involves the use of COMSOL multiphysics Finite Element software to develop an integrated electrical, thermal model with 3 micro meter water bubble radius. The presence of water tree results in the reduction of their dielectric strength. Here the Finite Element simulation technique is used to 11kV and 20kV power cables. A model that illustrates the water-dielectric interface within the cable insulation system is proposed.

**Keywords:** power cable, FEM, comsol multiphysics, electric field and temperature

**Copyright © 2014 Institute of Advanced Engineering and Science. All rights reserved.**

## 1. Introduction

Electric power system reliability start from generating, transmission comes up with distribution. At present, the power cable acts as the key role in power transmission. To operate cable networks for power transmission knowledge is needed of the maximum current load that can be applied without damage resulting to the cable. Underground construction could be a reasonable alternative to overhead in urban areas, where an overhead line cannot be installed with appropriate clearance, at any cost. In suburban areas, aesthetic issues, weather-related outages, some environmental concerns, and the high cost of some ROWs could make an underground option more attractive. These construction limitations often increase the cost of the project [1]. The trenching for the construction of underground lines causes greater soil disturbance than overhead lines. Overhead line construction disturbs the soil mostly at the site of each transmission pole. The presence of water within the insulation materials can only lead to forming water trees if a sufficient electric field exists. Therefore, many works have indicated that the initiation of water tree depends on the magnitude of electric trees and water availability [2].

In the present work, a model for medium voltage power cable is described based on the FE technique. This model comprises regions of insulation material and water particles with elliptical geometric structure for field and thermal model. The field enhancement as a function of sharpness of water particles is determined. The potential and field strength values throughout the insulation are calculated for cable under wet condition. The thermal model comprises temperature distribution throughout the cable structure. The significance of the simulation techniques in comparison with the actual experimental methods is highlighted. Finally, the results are used to demonstrate the mechanisms responsible for tree initiation and growth, which could be developed to cause breakdown inside the cable insulation.

## 2. Research method

### 2.1. Comsol Multiphysics Software

Two-dimensional COMSOL MULTIPHYSICS software was used in the present study. This Software provides automatic mesh generation for solving electrostatic, electromagnetic and Heat transfer problems by a differential operator FE method. The computational properties of the COMSOL are enabled.

- a) field and potential values at any boundary to be plotted,
- b) the display of equipotential and field lines in meshed regions.

Detailed description of FE formulation principles and procedures can be found in the user manual of such a package is available in paper [3]. In our case two modules are used those are electrostatic and heat transfer module because electrostatic module consist of electric field and potential models and heat transfer module consist of temperature distribution in a cable.

Figure 1. Flow Chart for COMSOL Multiphysics for Obtaining Solution

## 2.2. System Configuration

In order to study the electric field, potential and temperature distribution characteristics in cable insulation, the Comsol Multiphysics FE computer software is used to build a two-dimensional model for the cables under study as the investigated field lines are perpendicular to equipotential lines and directed from conductor to the outer sheath of the cable, a section made across the cable can illustrate the circumference and sharp edges of the ellipsoids aligned along these field lines [4].

Table 1. Cable Parameters

Voltage(kv)	Conductor Radius(mm)	Insulation thickness(mm)
11	3.9088	5.897
20	2.4333	1.456

The investigation of field development at the ellipse sides and the determination of its enhancement at the sharp ends of the ellipsoids are achieved by inspecting the field distribution on the plane of cable section. The lateral component of electric field around the ellipsoid surface, which penetrates the cable depth has less value than that at the horizontal ellipsoid edges. The cable configurations used in the three case studies are tabulated in Table 1 shown above [4]. Each cable comprises of an inner Copper conductor and outer insulation of paper which has a permittivity of 3.6. It has been reported that the amount of water, which can be absorbed by cable insulation, varies in the range 2-6% of the total insulation volume [5], and in the present analysis, the absorption was taken to be 3%. The radius of the spherical water droplet varies in the range of 0.1 to 5 $\mu$ m [6]. It is taken here to be 3 $\mu$ m.

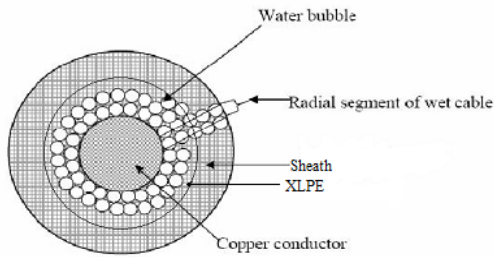


Figure 2. Proposed Model of Water Content in the Single Phase Power Cable

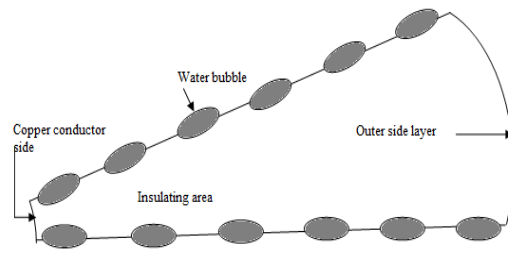


Figure 3. Proposed Model of Water Content in the Single Phase Power Cable

The computation of electric field distribution, it is arrogated that the water bubbles are distributed radially along the lines emanating from the conductor surface to the outer surface of insulation, as demonstrated in Figure 2. If it is arrogated that the elongation of water void to form an ellipse does not alter its area, the number of water voids per radial line can be ciphered as indicated in Table 3. These numbers also satisfy the condition that bubbles adjacent to cable conductor and subsequent bubbles in the insulation will not overlap. Figure 3 depicts how these bubbles are arranged to form sections of cable insulation restricted between pairs of rows of water voids. On the other hand, the electrostatic field analysis is simplified using this symmetrical model in which the total number of nodes and the triangular elements.

Table 2. Water Void Configuration

Voltage(kV)	Bubble Radius(μm)	Water Voids	Voids/radial line	Elements generated
11	5μm	145275	23	3495
20	5μm	230021	38	6212

To facilitate computation of electric field distribution, it is assumed that the water bubbles are distributed radially along the lines emanating from the conductor surface to the outer surface of insulation, as demonstrated in Figure 2. If it is assumed that the elongation of water particle to form an ellipse does not alter its area, the number of water bubbles per radial line,  $N_p$  can be calculated from Equation (1). Equation (2) gives the area of ellipse, which is assumed to be equivalent to a circular area of water bubble.

$$N_p = \frac{0.5DM(R^2 - r^2)}{r_{wp}^2} \tag{1}$$

$$\text{Area of ellipse} = \pi ab \tag{2}$$

Where  $R$  is the outer radius of the cable;  $r$  is the radius of the conductor;  $M$  is the percentage of absorbed water;  $r_{wp}$  the radius of the water particle;  $a$  and  $b$  are the major and minor axes of the elliptical shaped water particle. The parameter  $D$  is reported as a proportional value, relating that part of the circle restricted between two adjacent radial lines to the whole circle

According to the quoted values of conductor radius and insulation thickness above, the number of water bubbles in each line is varied. This number also satisfies the condition that bubbles adjacent to cable conductor and subsequent bubbles in the insulation will not overlap.

The difference in the dimensions of the water bubbles and the surrounding dielectric, containing these bubbles, is significant. This mismatch in dimensions actually leads to some inconvenience in the illustration of the studied model and in the selection of the accurate subdivisions during meshing process of various regions of the model. The Figure 4 shows all water bubbles along with the radial line and individual elliptical water bubble shape consisting of minor and major axis.

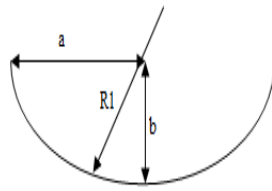


Figure 4. Elliptical Shape of Water Bubble

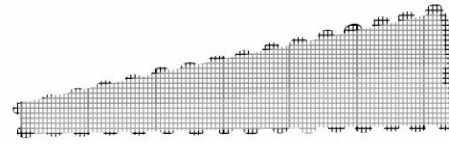
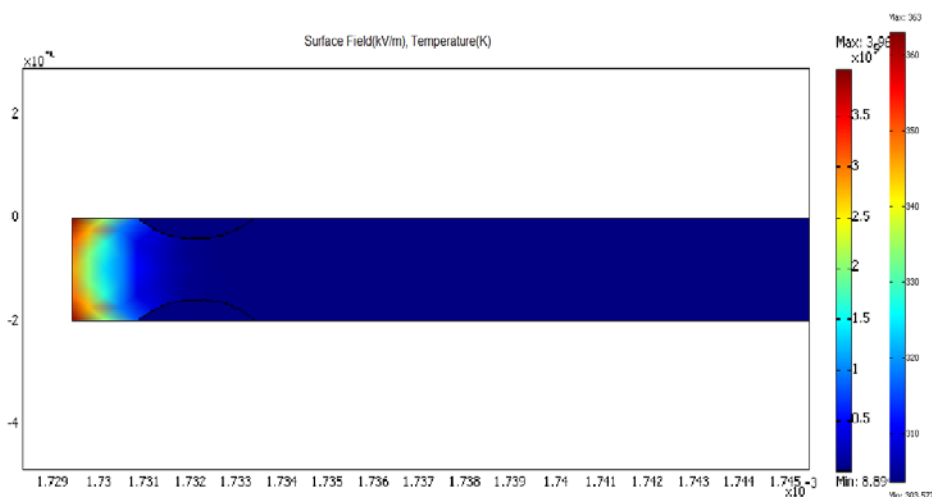


Figure 5. Computational Segment for FE Simulation

### 3. Results and Discussion

When the insulation system is free of water, the potential and field values have been decreasing in unequal steps from the conductor surface to the cable outer sheath. However, when the water particles are included within the insulation area, the field and equipotential lines show more divergence compared with the dry case. This non uniform distribution of field and equipotential lines becomes more noticeable at the dielectric-water interface, as the permittivity of the water is significantly greater than the dielectric.

When the water voids are sneaked in the cable insulation, the electric field at the tips of elliptically shaped water particles will be much higher. With a relative permittivity of water  $\epsilon_r = 80$  [6] compared with the cable insulation permittivity ( $\epsilon_r = 3.6$ ) it is expected to find that the field is heavily distorted in the vicinity of water bubble. To investigate the influence of the electric field distribution on the wet insulation of the cable, it was necessary to concentrate on one elliptical shape of water particles. The magnitude of the electric field was calculated for a number of points located in the symmetrical section. There are several factors which will determine the thermal behavior of a given cable installation. These include the assumed ampacity, the cable construction and circumstances of installation, the thermal properties of the surrounding soil and the ambient temperature. The principal heat source in the problem is the Joule heat dissipated in the conductor(s). The transfer of this heat to the surroundings is governed by the geometry and material properties of the conductor, insulation, screening, sheathing and trench fill materials as well as the ambient conditions are shown in Figure 6. The thermal and electrical systems are coupled via the temperature dependence of the resistivities of the conductor and sheath materials [7].

Figure 6. Field and Temperature Distribution in Wet Cable for 11kV Water Bubble Radius  $5\mu\text{m}$ 

In the normal operation of a cable, the heat loss, if any, is disregarded. However, the thermal instability, being a consequence of mismatch between steady state heat developed and dissipated, appears to be sensitive to omission of heat input function. The complexity arising out

of the inclusion of this additional term is, admittedly, considerable. However, in order to be able to compute the temperature distribution to a higher degree of accuracy, it becomes necessary to take into account the heat input function despite mathematical complexity [10].

**3.1. General Discussion**

The Electric field and thermal properties of wet cable is plotted here for two cases they Are:

- a) 11kV operating voltage, 5 micro meter Radius of water bubble.
- b) 20kV operating voltage, 5 micro meter Radius of water bubble.

The plots are plotted for each case considering:

- a) Electric field, potential and temperature distribution along the Curve line connecting number of water bubbles.
- b) Electric field, potential and temperature distribution inside the water bubble curve.
- c) Electric field, potential and temperature distribution along the Radial line of water bubble

**3.2. Electric Field, Potential and Temperature Distribution along the Curve Line Connecting Number of Water Bubbles**

**Potential (kV)**

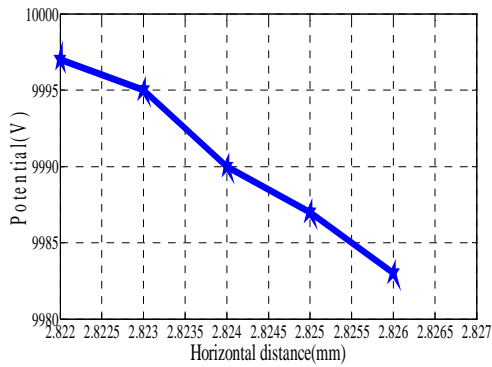


Figure 7.a. Electric Potential Distribution along the Curve Connecting Number of Water Bubbles 11kV

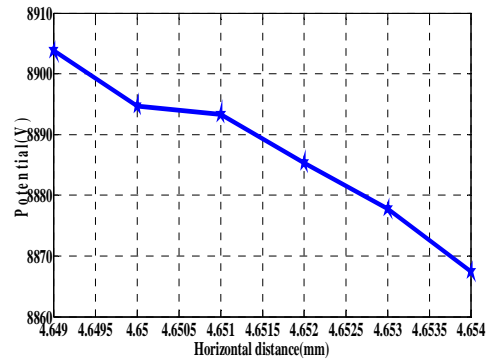


Figure 7.b. Electric Potential Distribution along the Curve Connecting Number of Water Bubbles 20kV

**Field (kV/m)**

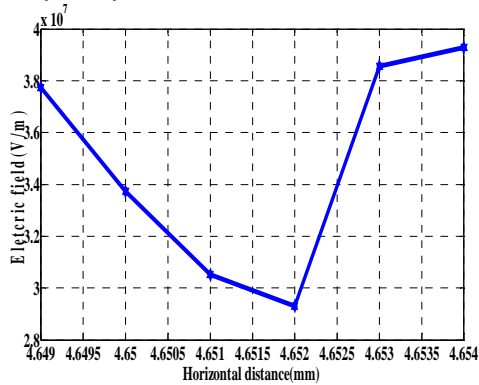


Figure 8.a. Electric Field Distribution along the Curve Connecting Number of Water Bubbles 11kV

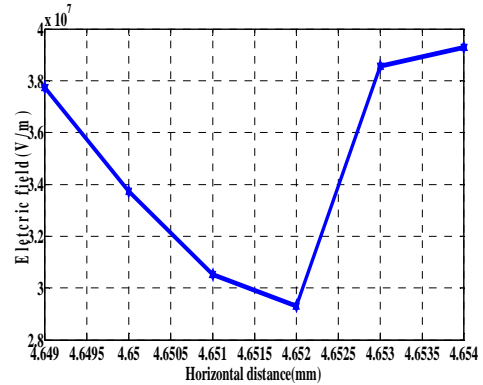


Figure 8.b. Electric Field Distribution along the Curve Line Connecting Number of Water Bubbles 20kV

Figure 7.a, 7.b and 8.a 8.b illustrate the values of electric field, potential and temperature along the radial line connecting a number of water bubbles. The radially lined water voids computed along the line connecting the water bubbles for 11kV and 20kV, 5µm voltage ratings for case 1. By observing these plots the field is maximum at conductor surface and then decreases towards water bubble and the plots are plotted with respect to horizontal distance from conductor to the sheath. Because the electric field varies with respect to distance i.e. electric field is inversely proportional to the distance [22] similarly for potential and temperature, in plot base-a indicates 11kV and base -b indicates 20kV.

**Temperature (K)**

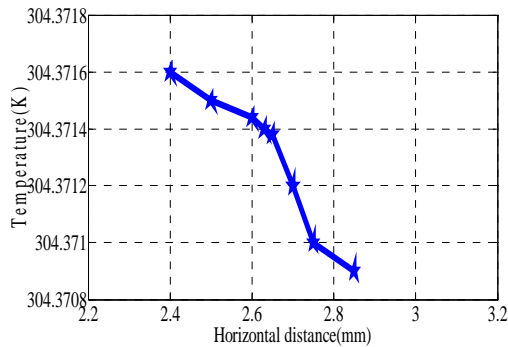


Figure 9.a. Temperature Distribution along Curve Connecting Number of Water Bubbles 11kV

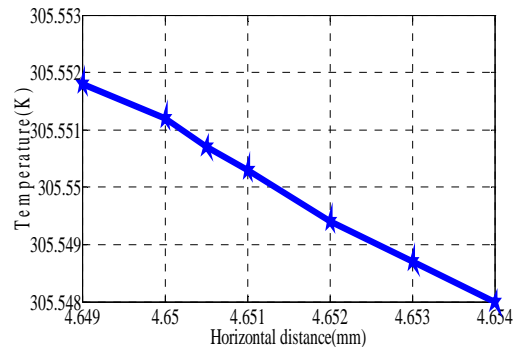


Figure 9.b. Temperature Distribution along the Curve Connecting Number of Water Bubbles 20kV

The temperature distribution from conductor surface to the radial line connecting water bubble is illustrated in Figure 9.a and 9.b. The temperature at the vicinity of the water particles is greatly intensified compared with that at the same location when the water particles are absent. The maximum boundary condition of temperature at conductor surface is 363K and outer sheath temperature is 293K.

**3.3. Electric Field, Potential and Temperature Distribution along Inside the Water Bubbles**

The electric field distribution, potential and temperature inside the water bubble are higher initially and then decreases with small change because the distance variation is in micro meters. Here for different cases numbers of water bubbles are varied depends on water bubble radius thus electric field, potential and temperature is calculated inside the bubble. Thus the change in Potential, field and Temperature is shown in Figure 10.a, 10.b and 11.a, 11.b.

**Potential (V)**

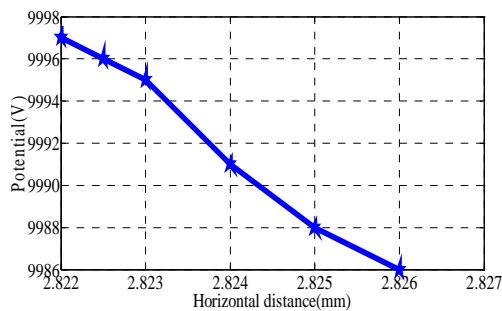


Figure 10.a. Electric Potential Distribution along Inside the Water Bubbles 11kV

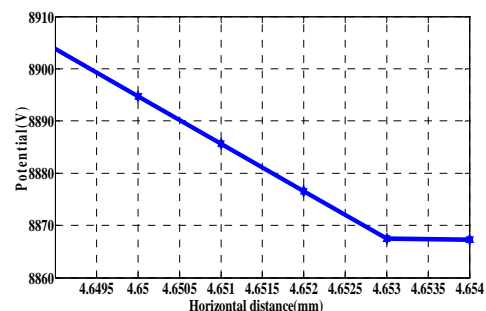


Figure 10.b. Electric Potential Distribution along Inside the Water Bubbles 20kV

**Field (kV/m)**

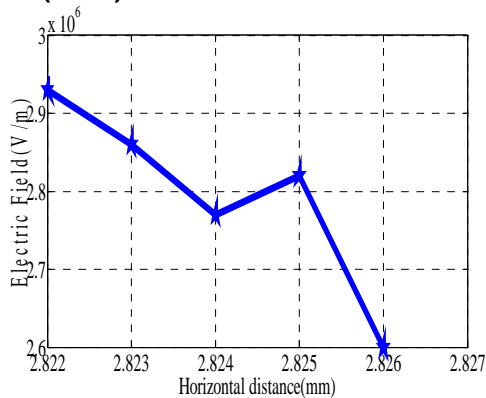


Figure 11.a. Electric Field Distribution along Inside the Water Bubbles 11kV

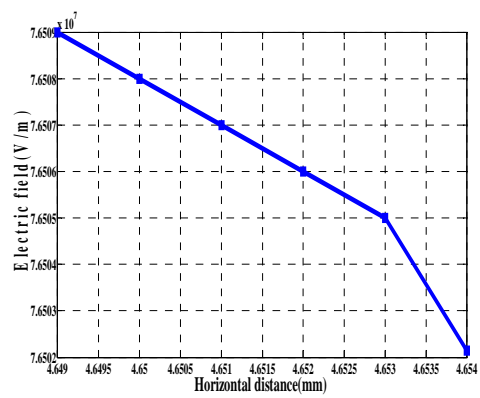


Figure 11.b. Electric Field Distribution along Inside Water Bubbles 20kV

The temperature distribution along water bubble is illustrates in Figure 12.a and 12.b. The temperature at the conductor surface to the first water bubble is more compare with temperature along water bubble curve i.e. variations in temperature is very less. The maximum boundary condition of temperature at conductor surface is 363K and outer sheath temperature is 293K so the temperature is in the range of 328K in this case.

**Temperature (K)**

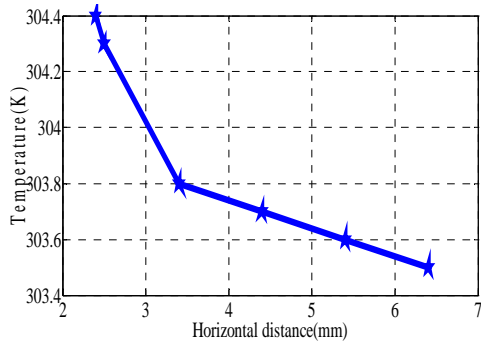


Figure 12.a. Temperature Distribution along Inside the Water Bubbles 11kV

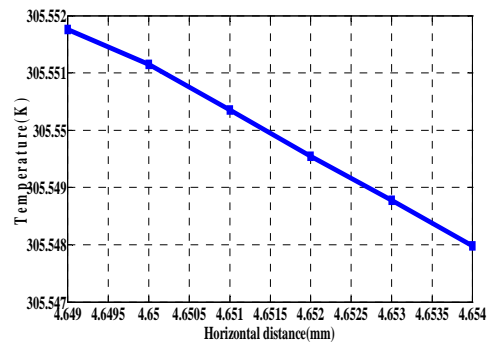


Figure 12.b. Temperature Distribution along Inside the Water Bubbles 20kV

**3.4. Electric Field, Potential and Temperature Distribution along the Radial Line Water Bubbles**

The regions located in the vicinity of the sharp edges of the water particles, especially those close to the conductor surface and characterized by a high field are suitable points for tree initiation. The growth of such trees means a high field will be originated at the tip of the structural channels of these trees, which can inevitably affect those low field areas with time. If the water absorption process continues, the number of water particles will increase and consequently the number of high-field regions also increases. The electric field distribution from conductor surface is higher compare with electric field along the tip of the water bubble. Here for different cases number of water bubbles is varied depends on water bubble Radius thus electric field is calculated each end point of every bubble i.e. tip of the water bubble. Initially at conductor surface is higher for every water bubble field distributes with gradual change. Thus the change in field and potential is shown in Figure 13, 14, 15, 16 and 17.

**Potential (V):**

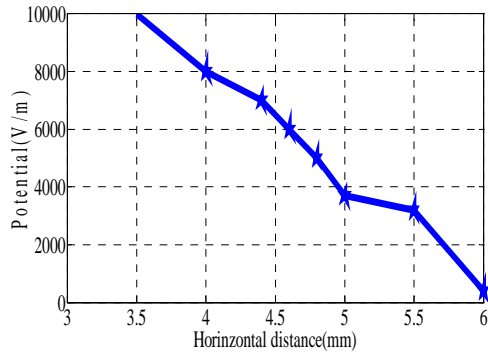


Figure 13. Electric Potential Distribution along the Radial Line Connecting Number of Water Bubbles 11kV

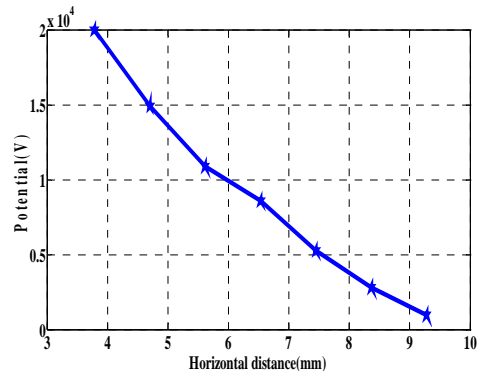


Figure 14. Electric Potential Distribution along the Radial Line Connecting Number of Water Bubbles 20kV

**Field (kV/m)**

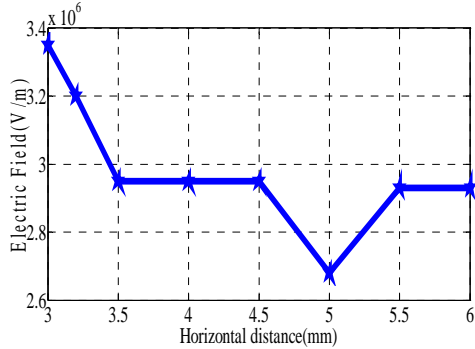


Figure 15. Electric Field Distribution along the Radial Line Connecting Number of Water Bubbles 11kV

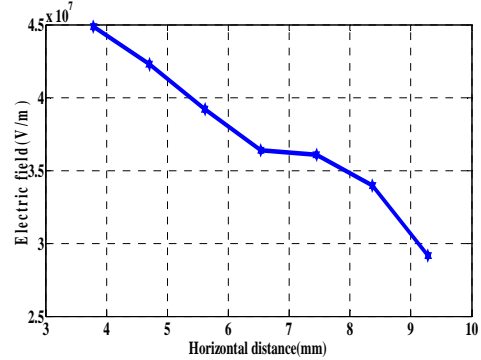


Figure 16. Electric Field Distribution along the Radial Line Connecting Number of Water Bubbles 20kV

**Temperature (K)**

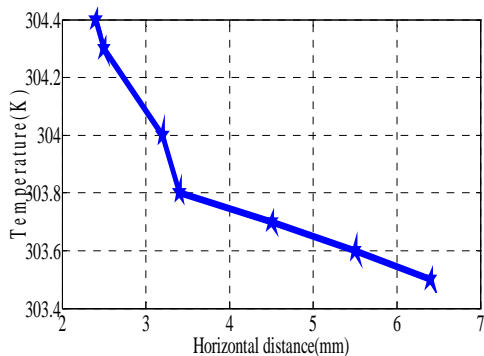


Figure 17. Temperature Distribution along the Radial Line Connecting Number of Water Bubbles 11kV

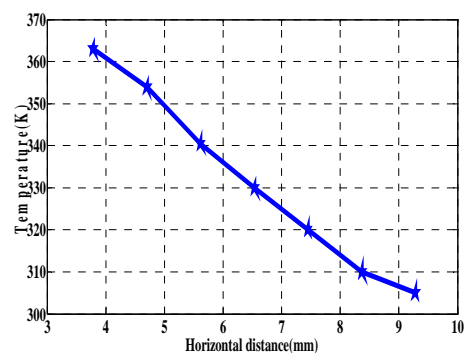


Figure 18. Temperature Distribution along the Radial Line Connecting Number of Water Bubbles 20kV

The temperature distribution from conductor surface to the radial line connecting water bubble is illustrated in Figure 17 and 18. The temperature at the vicinity of the water particles is greatly intensified compared with that at the same location when the water particles are absent. The maximum boundary condition of temperature at conductor surface is 363K and outer sheath temperature is 293K.

#### 4. Conclusion

In this paper a study of electric field, electric potential and temperature distribution in wet cable insulation for 11kV and 20kV power cable are endeavored using two-dimensional finite element based models of the power cables. These models were used to compute the electric field and temperature distribution inside the insulation and the field enhancement at the tips of elliptical water particles. According to the results, we can see that the temperature in the conductor core of cable is more. This is due to the power losses in the conductor. The temperature decreases when we come to the outer sheath of the cable. It is showed that the highest distribution in the conductor while the cable insulation near grounded showed lower distribution of temperature as according to given boundary condition. It was ascertained that the field enhancement is strongly subordinated upon the shape and absorbed water particles. Eventually, the role of electric field in the power cable and the possible mechanisms of the insulation aging and break down due to water infestations are briefly addressed.

#### References

- [1] Peter A Wallace, Donald M Hepburn, Chengke ZHOU, Mohamed Alsharif. *Thermal response of a three core belted pilc cable under varying load conditions*. CIREC 20th International Conference on Electricity Distribution Prague. 2009: 8-11.
- [2] *Underground Electric Transmission Lines*. Public Service Commission of Wisconsin. Madison, WI 53707-7854. 1-22
- [3] HSB Elayyan, MH Abderrazzaq. Electric Field Computation in Wet Cable Insulation Using Finite Element Approach. *IEEE Transactions on Dielectrics and Electrical Insulation*. 2005; 129(6): 1125-1133.
- [4] Salama Manjang, Bidayatul Arminyah. The radial distribution of temperature in xlpe cable an analysis the finite element numerical method. *IEEE*. 2006; 439-445.
- [5] Yanmu LI, LIANG Yongchun LI, Yanming, SI, Wenrong, YUAN Peng LI, Junhao. *Coupled Electromagnetic-Thermal Modeling the Temperature Distribution of XLPE Cable*. *IEEE*. 2009.
- [6] COMSOL Group Ltd., Stockholm, Sweden. *Comsol MultiPhysics Software package*. Version 3.2a. 2006.
- [7] William A Thue *Washington, DC marcel d'ekkerin*. *Electrical Power Cable engineering*. Copyright © 1999 by Marcel Dekker, Inc.
- [8] G Buonanno, A Carotenuto, M Dell'Isola, D Villacci. *Effect of radiative and convective heat transfer on thermal transients in power cables*. *IEEE Proc.-Gener. Transm. Distrib.*, 1995; 142: 436-444.
- [9] JH nehar, MH McGrath. *The calculation of the temperature rise and load capability of cable systems*. *AIEEE transaction part-III –power apparatus systems*. 1957; 76: 752-772.
- [10] Carlos Garrido, Antonio F Otero, Jose Cidras. *Theoretical Model to Calculate Steady-State and Transient Ampacity and Temperature in Buried Cables*. *IEEE Transactions on Power Delivery*. 2003; 18: 667-677.
- [11] P Werelius, P Thaming, R Erikson, B Holmgren, U Gafvertet. Dielectric Spectroscopy for Diagnosis of Water Tree Deterioration in XLPE Cables. *IEEE Trans. Dielectr. Electr. Insul.* 2001; 8:a 2742,
- [12] Reddy. *An Introduction to the Finite Element Method*. J.N. 1984, Mc-Graw Hill Book Company, New York.
- [13] IEC Standard 1982. *Calculation of the Continuous Current Rating of Cable (100% load factor)*, Publication 287.
- [14] Istardi D, Triwinarko A. *Induction Heating Process Design Using COMSOL® Multi Physics Software*.
- [15] K Rajagopala, K Panduranga Vittal, Hemsingh Lunavath. Electric Field and Thermal Properties of wet Cable. *TELKOMNIKA Indonesian Journal of Electrical Engineering*. 2012; 10(7): 1904-1916.